

Figure 2: Phase space distribution of the electron beam after collision (top) and the evolution of the electron beam size and emittance (bottom) for  $d_e = 27$ . In the top figure, the rms and 6 rms ellipses for both geometric and effective emittance, respectively, are plotted.

We use simulation code, EPIC[3], to calculate the electron beam evolution inside the opposing ion beam. Figure 2 and 3 illustrate the examples of the electron beam distribution after the collision and the e-beam evolution inside the ion beam. The former correspond to the case of  $d_e = 27$ , and latter for  $d_e = 150$ . In the electron beam distribution plots, the nonlinear force deform its initial Gaussian distribution completely. The electrons with larger betatron amplitude rotate slower than those in the core. Therefore the distribution after collision forms a spiral shape. We use 2 different definitions of beam emittance to characterize the occupied phase space area. One is the rms geometric emittance obtained from the beam distribution, written as:

$$\varepsilon_x = \sqrt{\langle (x - \bar{x})^2 \rangle \langle (x' - \bar{x}')^2 \rangle - \langle (x - \bar{x})(x' - \bar{x}') \rangle^2} \quad (1)$$

The other emittance takes the design optics function into account and is name effective emittance. It is defined as the half of the average value of Courant-Snyder invariant of all macro-particles based on design lattice:

$$C(\tilde{x}, \tilde{x}') = \gamma \tilde{x}^2 + 2\alpha \tilde{x} \tilde{x}' + \beta \tilde{x}'^2 \quad (2)$$

In the e-beam distribution plots of figure 2 and 3, both

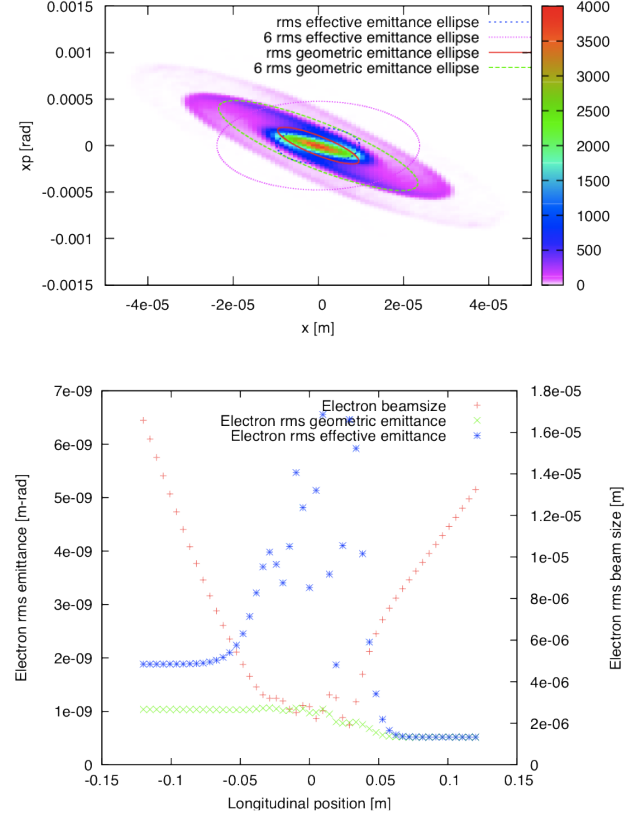


Figure 3: Phase space distribution of the electron beam after collision (top) and the evolution of the electron beam size and emittance (bottom) for  $d_e = 150$ . In the top figure, the rms and 6rms ellipses for both geometric and effective emittance, respectively, are plotted.

emittances are represented as ellipses of one rms value and 6 rms value. The evolution plots illustrate the evolution of the two rms emittance and the rms beam size. These plots clearly show the mismatch between the beam distribution and the design optics due to the beam-beam interaction. The effective emittance will determine the aperture requirement of the magnet downstream of interaction point (IP), as shown in figure 4. The calculated aperture shows that the small-gap magnet designed for eRHIC is suitable for the ERL energy recovery passes.

### 3 KINK INSTABILITY AND ITS MITIGATION METHODS

The kink instability develops due to the electron beam passes the imperfection of the head of the ion beam to its tail. Therefore, for the ion beam, the beam-beam interaction behaves as an effective wake field. If we assume both beams have only infinitesimal offsets, the wake field

$$W(s, s') = \frac{\gamma_i}{Z^2 N_{ib} r_i} \frac{\Delta x'(s)}{\Delta x(s')} \quad (3)$$

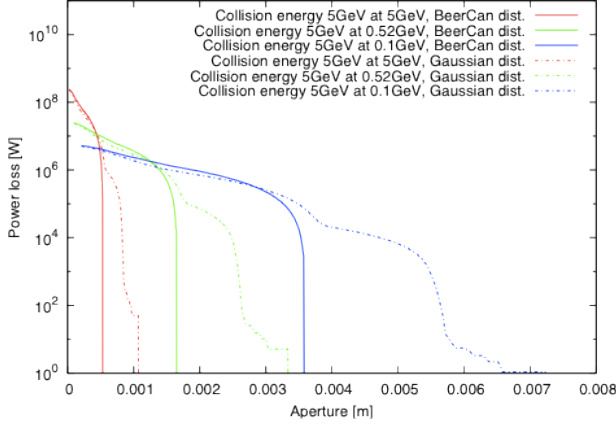


Figure 4: The aperture requirement of the energy recovery pass downstream IP. A maximum 10 meter  $\beta^*$  is assumed in all arcs.

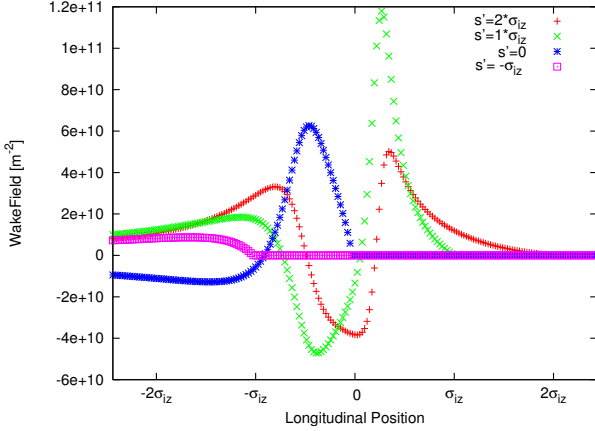


Figure 5: The example of the kink wake field with the beam-beam parameter of the ion beam  $\xi_p = 0.015$ . The electron beam has disruption parameter  $d_e = 27$ . In the figure, the electron beam travels from the positive  $s$  to negative.  $s'$  denotes the location of the introduced offset.

can be retrieved from simulation, where  $N_{ib}$  is the number of ions in the slice,  $\gamma_i$  is the energy of the ion beam and  $r_i$  is the classical radius of the ion beam. The wake field is illustrated in figure 5.

The threshold of the strong head-tail instability (the kink instability) can be calculated using the 2-particle model or the multi-particle model[4]. Both models are based on linearized beam-beam forces. For a 2-particle model, the threshold simply reads:  $\xi_i d_e < 4\nu_s/\pi$ . However, to model the electron beam correctly in high disruption parameter case, the multi-particle model should be used predicting the threshold as in figure 6.

Both linear models predict that the parameter of the eRHIC exceeds the threshold. A simulation using nonlinear beam-beam forces is required to confirm this understanding. Figure 7 shows the emittance growth associated with the kink instability at different disruption parameters of the

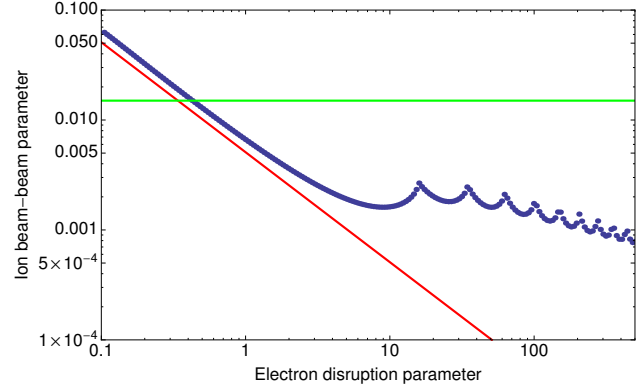


Figure 6: The threshold of kink instability, with the choice of the synchrotron tune 0.004. The Blue dots denotes the threshold calculated from 51 macro-particles circulant matrix method. The red line represents the simple threshold form from equation  $\xi_i d_e < 4\nu_s/\pi$ . The green line corresponds to  $\xi_i = 0.015$ , which is design beam-beam parameter of ion beam in eRHIC.

electron beam. Even with the lowest disruption parameter,  $d_e = 5$ , the system is not stable at +2 chromaticity (the nominal value of RHIC operation), although the emittance growth in this case is much less than those with higher  $d_e$ . If we increase the chromaticity to stabilize the emittance growth, it requires unreasonable values. Therefore, a dedicate feedback system is desired as a countermeasure.

The first feedback system[4], shown in figure 8, takes full advantage of flexibility of a linac-ring scheme, which has following procedures. We steer the fresh electron bunch before collision based on the transverse offset of the last-used electron bunch that collides with the same ion bunch. Then the centroid of the new electron bunch will oscillate within the opposing ion bunch due to the focusing beam-beam force. We are expecting that oscillation of the centroid of the electron bunch gives the ion bunch proper kicks to correct the offset of the ion bunch before the visible adverse effect, such as emittance growth and luminosity loss, due to the kink instability.

Mathematically, we introduce the offset by modifying the motion of the centroid of the electron bunch based on the information from the last one.

$$\begin{pmatrix} \bar{x}_e \\ \bar{x}'_e \end{pmatrix}_{n+1,i} = M_f \begin{pmatrix} \bar{x}_e \\ \bar{x}'_e \end{pmatrix}_{n,f} \quad (4)$$

Here, the subscript  $n$  denotes the electron-ion collision in  $n^{th}$  turn, the subscripts  $i$  and  $f$  respectively represent the bunch centroid before and after collision. Map  $M_f$  defines the algorithm of the feedback system. Here, we limit  $M_f$  to be a matrix for simplicity and easier realization.

Figure 9 shows the effect of this feedback system at disruption parameter 5. In this case, the emittance growth due to the kink instability is suppressed with proper amplitude of the feedback gain  $m_{11}$  (-0.01 or -0.02) without a noticeable decreasing in luminosity. An incorrect sign of the gain

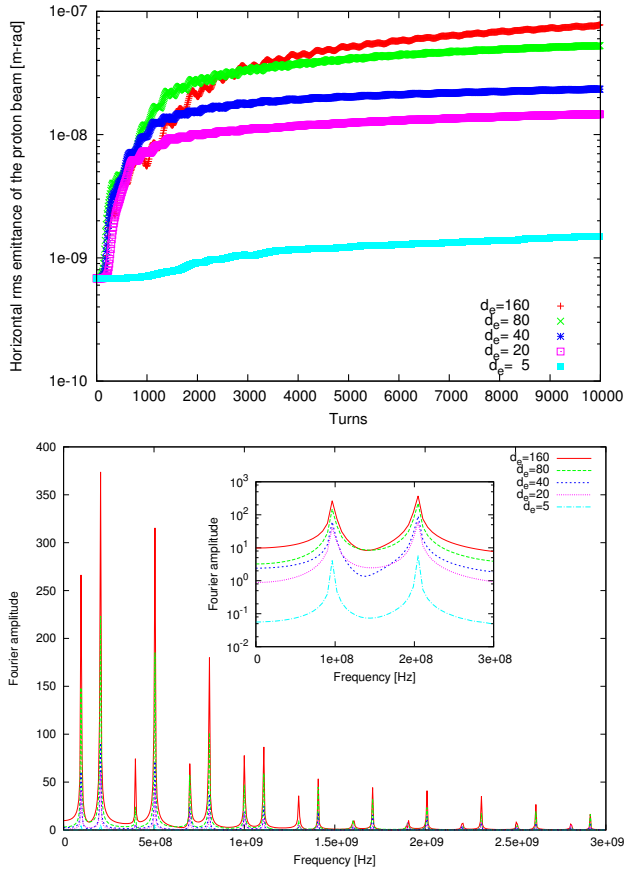


Figure 7: Top: The proton beam emittance growth due to the kink instability at different disruption parameters with the chromaticity of both transverse directions set at +2 units, and the beam-beam parameter of the proton beam at 0.015. Bottom: The Fourier spectrum of the turn by turn proton slice centroid data. The proton beam is cut to 100 longitudinal slices for this calculation.

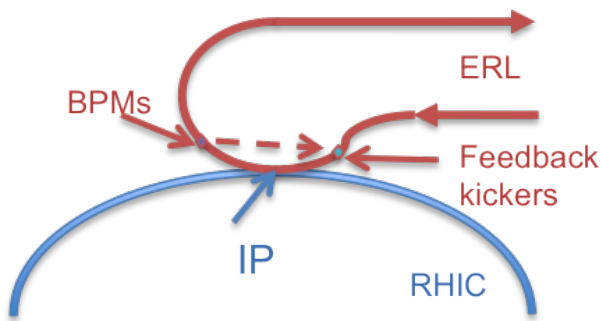


Figure 8: The schematic layout of the feedback system I for mitigating the kink instability in eRHIC.

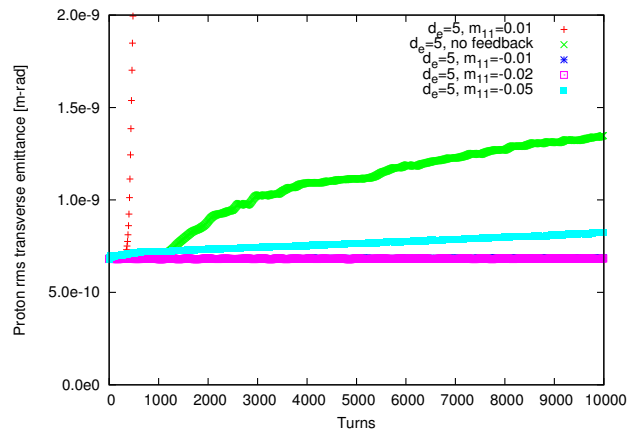


Figure 9: The effect of the feedback system at disruption parameter 5.

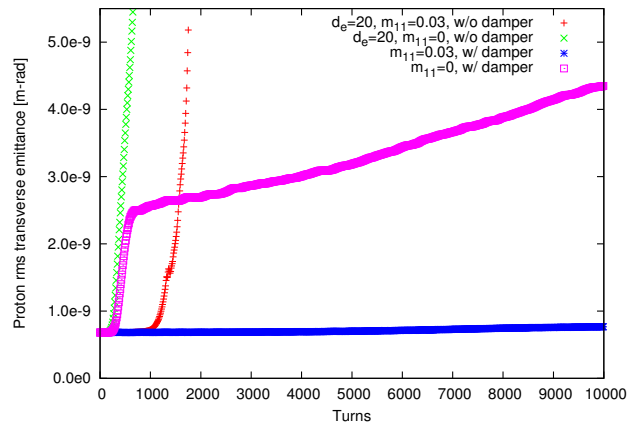


Figure 10: The effect of the feedback system at disruption parameter 20.

may boost the instability, as shown by the red dots in figure 9.

When the disruption parameter exceeds 15, this feedback system itself can not stabilized the emittance, because the system will excite the instability of the rigid mode while it can correct the head-tail mode of the ion beam. Therefore we have to add the transverse bunch-by-bunch damper to damp the rigid mode of the ion beam simultaneously. The result for  $d_e = 20$ , as an example, is shown in figure 10. The red dots shows the case with the feedback gain of  $m_{11} = 0.03$  without transverse damper. The centroid of the ion bunch becomes unstable and causes fast emittance growth due to the offset of two beams. By applying the bunch by bunch feedback in the simulation, the ion centroid is stable and the emittance growth is prevented (blue curve).

The simple feedback lose its efficiency when  $d_e > 25$ . In this range, the electron beam oscillate too fast and the frequency of the oscillation does not match that of the lowest instability mode. We need alternative feedback scheme for those disruption parameter range, such as a traditional

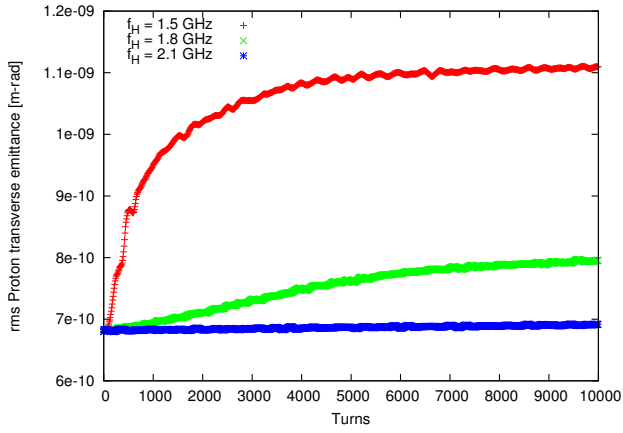


Figure 11: Comparison of kink instability damping with different high frequency limit  $f_H$  when disruption parameter  $d_e = 150$ . The gain of the feedback is selected to minimize the emittance growth ion beam.

pick-up and kicker system in the ion beam to suppress the instability coherently[5].

For the pickup-kicker system, the effect can also be modeled as a wake field. If we assume the system has a uniform frequency response with a low and high frequency limit  $f_L$  and  $f_H$ , the corresponding wake field of this system reads[6] :

$$W(\tau) = R \int_{f_L}^{f_H} \cos(2\pi f\tau) df \quad (5)$$

where  $R$  is related to gain of the amplifier between the pickup and the kicker.

We fix the low frequency limit to 50 MHz, which is below the first peak in bottom figure of 7. Then we vary the high frequency limit to find the requirement for individual disruption parameter.

Figure 11 shows that the required  $f_H$  is at least 2.1 GHz to suppress the kink instability when  $d_e$  is 150. For other  $d_e$ , as shown in figure 12, the required  $f_H$  is a monotonically increasing function of  $d_e$ . Therefore, we demonstrated that the kink instability will be suppressed by a pickup and kicker system with whole electron beam disruption parameter range (5-150), if required frequency bandwidth is selected.

#### 4 NOISE HEATING EFFECT OF THE ION BEAM

Since the ion beam always collides with fresh electron bunches, the electron beam parameter fluctuation will affect the ion beam through the beam-beam interaction. The fluctuations can be classified as two types. The first is dipole errors due to the electron beam transverse position offset; the second is quadrupole error due to the fluctuation of the electron beam intensity or transverse beam size.

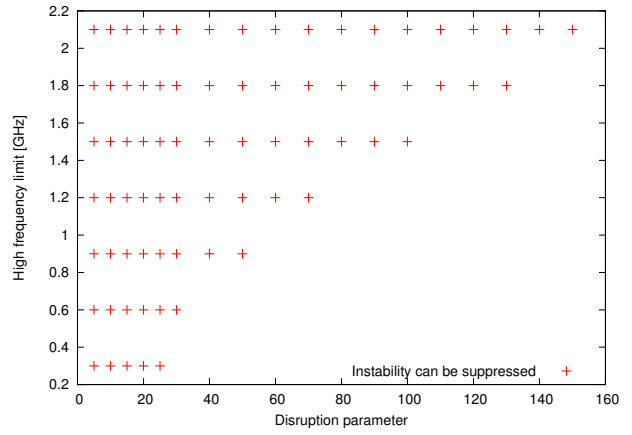


Figure 12: The relation between the required high frequency limit  $f_H$  and the electron disruption parameter  $d_e$ . Each point denote that the instability can be suppress in the corresponding parameter ( $f_H$  and  $d_e$ ) with proper amplitude. For all calculation, the low frequency limit is fix to 50 MHz

If the noise of the electron beam is considered as white noise, i.e. uniform spectrum in frequency domain, the effect of both dipole error and quadrupole errors can be evaluated analytically. For the quadrupole errors, the rms beam size of the ion beam is expected to grow exponentially, with the rising time

$$\tau = \frac{T}{4\pi^2 \xi_i^2} \frac{1}{(\delta f/f)^2}$$

where  $\xi_i$  is the beam-beam parameter of the ion beam,  $T$  is the revolution period and  $\delta f/f$  is the rms error of the beam-beam focal length. For eRHIC parameters, to get slow rising time ( $\sim 10$  hours), the relative error of electron beam parameter should be better than  $2 \times 10^{-4}$ . In reference [7], a Lorentz frequency spectrum  $g(\omega) = 1/(\omega^2 + \alpha^2 \omega_0^2)$  is considered, where  $\alpha$  is a free parameter much less than one and  $\omega_0$  is the angular revolution frequency of the ion ring. In this case, the rising time  $\tau$  is lengthened to  $\tau/R(\alpha)$ , where:

$$\begin{aligned} R(\alpha) &= \frac{1 - \exp(-2\alpha)}{1 + \exp(-2\alpha) - 2 \cos(4\pi\nu) \exp(-\alpha)} \\ &= \frac{\alpha}{1 - \cos(4\pi\nu)} + O(\alpha^3) \end{aligned}$$

For the dipole errors, the ion beam is kicked turn by turn due to the electron beam random offset. By following the well-known random walk formulas, the ion beam displacement gives  $\sqrt{\langle x_i^2 \rangle(t)} = \sqrt{t/\tau} + \langle x_i^2 \rangle(0)$  and  $1/\tau = 8\pi^2 \xi_i^2 \langle d_n^2 \rangle / T$ , where  $d_n$  is the  $n^{\text{th}}$  turn electron beam displacement at IP. We need a bunch by bunch transverse damper in the ion ring to compensate the dipole heating up effect.

## 5 CONCLUSION

We reports on the key finding for distinct beam-beam effects in the ERL based eRHIC. Our study identified the challenges and well as possible countermeasures for both the electron and the ion beams.

A dedicated feedback system is required to suppress the emittance growth caused by the kink instability. We proposed two possible feedback systems. The feedback applied to the electron beam works for moderate values of disruptionParameter, e.g.  $d_e < 25$ . A traditional broad-band pickup and kicker feedback system can damp the instability for the whole range of disruption parameter expected in eRHIC.

We report on the requirement for the intensity and beam size stability of the electron beam to avoid the hadron beam emittance growth caused by noise in beam-beam interactions. We also established a need for a transverse bunch-by-bunch damper to compensate for possible heating effect caused by random noise in transverse displacement in the electron beam.

## 6 REFERENCES

- [1] V. Ptitsyn and et. al, eRHIC Accelerator Position Paper, Tech. Rep. (C-AD, BNL, 2007).
- [2] Y. Hao and V. Ptitsyn, Phys. Rev. ST Accel. Beams 13, 071003 (2010)
- [3] Y. Hao, Beam-Beam Interaction Study in ERL based eRHIC, Ph.D. thesis, Indiana University (2008).
- [4] Y. Hao, et. al., "Feedback Scheme For Kink Instability in ERL Based Electron Ion Collider", Proceedings of 2011 Particle Accelerator Conference, New York, NY, USA
- [5] Y. Hao, et. al., "Kink Instability Suppression with Stochastic Cooling Pickup and Kicker", Proceedings of 2012 International Particle Accelerator Conference, New Orleans, NM, USA
- [6] M. Blaskiewicz and J.M. Brennan, WEM2105, in Proceedings of COOL 2007, Bad Kreuznach, Germany
- [7] M. Blaskiewicz, "Emittance Growth from Electron Beam Modulation", C-A/AP/#363, December 2009